

# PERFORMANCE COMPARISON OF COMPUTATIONAL RETINA MODELS

João C. Martins  
Escola Superior de Tecnologia e Gestão/INESC-ID  
Instituto Politécnico de Beja  
Av. Afonso III  
7800-050 Beja, Portugal  
email: Joao.Martins@estig.ipbeja.pt

Leonel A. Sousa  
Instituto Superior Técnico/INESC-ID  
Universidade Técnica de Lisboa  
Av. Rovisco Pais  
1049-001 Lisboa, Portugal  
email: las@inesc-id.pt

## ABSTRACT

A comparative study of bio-inspired computational retina models, representative of two distinct model classes, is presented in this paper. One model belongs to the so called class of pseudo-deterministic models, where a given light stimulus always produces the same response, while the other analyzed model belongs to the stochastic class and mimics the random behavior of the retina response. Both the firing rate and spike train metrics are used to evaluate and compare both models. Experimental results, obtained with real data, show that the two models present similar outcomes, despite their distinct nature, although there is a slightly better performance of the pseudo-deterministic model in practice.

## KEY WORDS

Retina models. Computational models. Visual image processing. Error measures.

## 1 Introduction

The science enterprise of conveying vision to blind people is, nowadays, a demanding and challenging task. The quest for developing prosthesis for the profoundly blind people is refrained not due to technological issues, since with today's computers and electronics it is virtually possible to engineer any apparatus that the human kind can imagine. The difficulty is instead related to the human brain with all its complex neuronal processing capabilities of extracting reliable information from a bunch of apparently incoherent sequence of evoked potentials, vulgarly called spikes, and is considered to be one of the last science frontiers.

In the demand for a retina model two distinct features, related to the interpretation of the spike train elicited by a given visual stimulus, should be considered. The first is the fact that the presentation of the same visual stimulus result in different spike trains, what is called variability, and the second is that different light stimulus can originate similar spike responses, a fact called ambiguity [1]. These facts preclude a correspondence from one to one between the light stimulus and the retina response, making evident that the retina presents a nonlinear behavior [2].

A prior question is what information is coded by the spike train and how is that information encoded [3]. Although this question is not undoubtedly answered, physiologists already know what are the most important features of the spike train that convey information [4] [5]. Several studies point out that the time occurrence of the first spike, the number of spikes, and the time lag between the first and second spikes in a giving firing event, convey the major part of the information in the spike train [6]. As an ultimate goal, a successful retina model should try to approximate the answer of a real retina within the variability of the neural code.

Several models have been proposed to resemble the retina behavior in response to distinct classes of light stimulus [7]. In this paper two of the most recent proposed models, belonging to distinct classes, are analyzed. The first is a pseudo-deterministic model [8], where a given light stimulus produces always the same model output, corresponding to the firing rate, and a posterior spike generator is included to generate the spike train. The second model belongs to the class of stochastic models [9], where noise is introduced within the model to resemble the spike train variability. This paper tries, for the first time, to experimentally evaluate and compare these two different types of retina models based on real data. As it can be observed from this paper this is not a trivial task, since the models provide different types of outputs and because we are trying to precisely compare information that is stochastic at the base. This preliminary study leads to the important conclusion that the models produce good results in response to a sequence of spatially uniform images, regardless of the different used problem approach.

This paper is organized as follows. Section 2 describes the retina models considered in this paper. In Section 3 the models are analyzed and experimental results are presented. Finally, Section 4 concludes the paper.

## 2 Retina Models

### 2.1 The Pseudo-Deterministic Model

The pseudo-deterministic retina model has the block structure depicted in Figure 1.

The signal  $s(\mathbf{r}, t)$  represents the light stimulus pattern

---

This work was partially supported by FCT under the project POSI/EEA-CPS/61779/2004

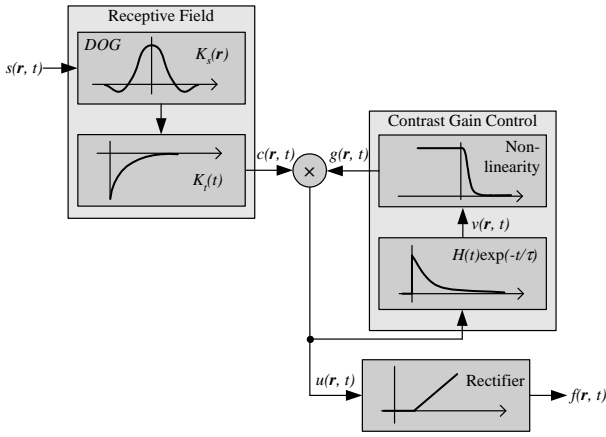


Figure 1. Pseudo-deterministic model.

that hits the retina, as a function of time  $t$  and space  $\mathbf{r}$ , where  $\mathbf{r}$  is the position vector  $\mathbf{r} = (x, y)$ . The first major block of the model resembles the receptive field of the ganglion cell (RF), where the spatiotemporal stimulus pattern is convolved with a kernel function  $K(\mathbf{r}, t)$ , resulting in the activation signal of the ganglion cell:  $c(\mathbf{r}, t)$ . This kernel operation is described by the convolution

$$c(\mathbf{r}, t) = K(\mathbf{r}, t) * s(\mathbf{r}, t - \Delta t) \quad (1)$$

where  $\Delta t$  is the response latency. For the receptive fields of retina ganglion cells this kernel can be separated, with a good approximation, in a time and a space kernel [10], so it can be factorized into spatial and temporal parts like

$$K(\mathbf{r}, t) = K_s(\mathbf{r}) K_t(t) \quad (2)$$

For the space factor it is used a difference of Gaussians (DoG), that simulates the receptive field properties of the retinal ganglion cells [10], with expression

$$K_s(\mathbf{r}) = \frac{w_C}{2\pi\sigma_C^2} \exp\left(\frac{-\mathbf{r}^2}{2\sigma_C^2}\right) - \frac{w_S}{2\pi\sigma_S^2} \exp\left(\frac{-\mathbf{r}^2}{2\sigma_S^2}\right) \quad (3)$$

The parameters  $w_C$  and  $w_S$  give the weight of the receptive field center against its surround, respectively. On the other hand, the parameters  $\sigma_C^2$  and  $\sigma_S^2 = \beta^2\sigma_C^2$  (with  $\beta > 1$ ) control the diameter of the center and surround Gaussian functions, respectively.

The temporal factor have the expression

$$K_t(t) = \delta(t) - \alpha H(t) \exp(-\alpha t) \quad (4)$$

corresponding to a high-pass filter which impulse response has a time decay of  $1/\alpha$ , and where  $H(t)$  is the Heaviside step function.

The feedback loop of the model consists of, what is called, a contrast gain control (CGC) [11], inserted to capture the characteristics of the retinal response. The signals  $c(\mathbf{r}, t)$  and  $g(\mathbf{r}, t)$  are multiplied, giving the neuron activation  $u(\mathbf{r}, t)$ :

$$u(\mathbf{r}, t) = g(\mathbf{r}, t)[K(\mathbf{r}, t) * s(\mathbf{r}, t - \Delta t)] \quad (5)$$

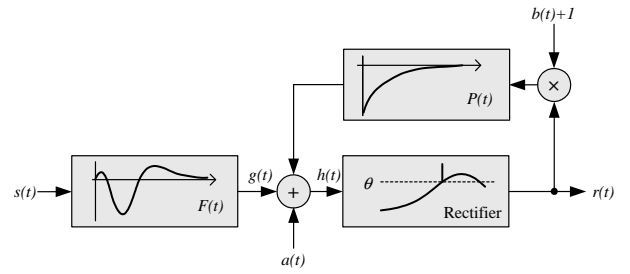


Figure 2. Stochastic model.

The CGC loop comprehends a low-pass temporal filtering integration of the neuron activation signal:

$$v(\mathbf{r}, t) = B u(\mathbf{r}, t) * [H(t) \exp(-t/\tau)] \quad (6)$$

where the parameter  $B$  controls the amplitude, and  $\tau$  the time duration of the integration, and a static nonlinearity with the form:

$$g(\mathbf{r}, t) = \frac{1}{1 + \{[v(\mathbf{r}, t)]_+\}^4} \quad (7)$$

where  $[x]_+ = x H(x)$  is the rectification operator and  $H()$  is the Heaviside function, resulting in a factor that modulates the receptive field output.

At the end, the neuron activation signal is rectified to obtain the instantaneous firing rate of the retinal ganglion cell,  $f(\mathbf{r}, t)$ . The rectification has the form

$$f(\mathbf{r}, t) = \tilde{\alpha}[u(\mathbf{r}, t) + \Theta]_+ \quad (8)$$

where  $\tilde{\alpha}$  establishes the scale and  $\Theta$  the baseline of the firing rate, respectively. When the stimulus  $s(\mathbf{r}, t)$  is static the activity signal  $u(\mathbf{r}, t)$  is zero and the neuron response is equal to the baseline activity:  $f(\mathbf{r}, t) = \tilde{\alpha}\Theta$ . This output firing rate was used to produce a spike train using a Poisson spike generator [12], introducing a random behavior but outside the model.

## 2.2 The Stochastic Model

The block structure of the stochastic model is presented in Figure 2.

Despite this model being only temporal, it can be extended to include a spatial treatment of the stimulus, particularly if it is assumed that the temporal and spatial stimulus processing can be separated, as it was done in the pseudo-deterministic model.

In Figure 2 the stimulus  $s(t)$  is filtered by the linear filter  $F(t)$  to produce the signal  $g(t)$ . The filter function  $F(t)$  is synthesized using a linear combination of orthonormal functions like

$$F(t) = \sum_{j=1}^N k_j f_j(t) \quad (9)$$

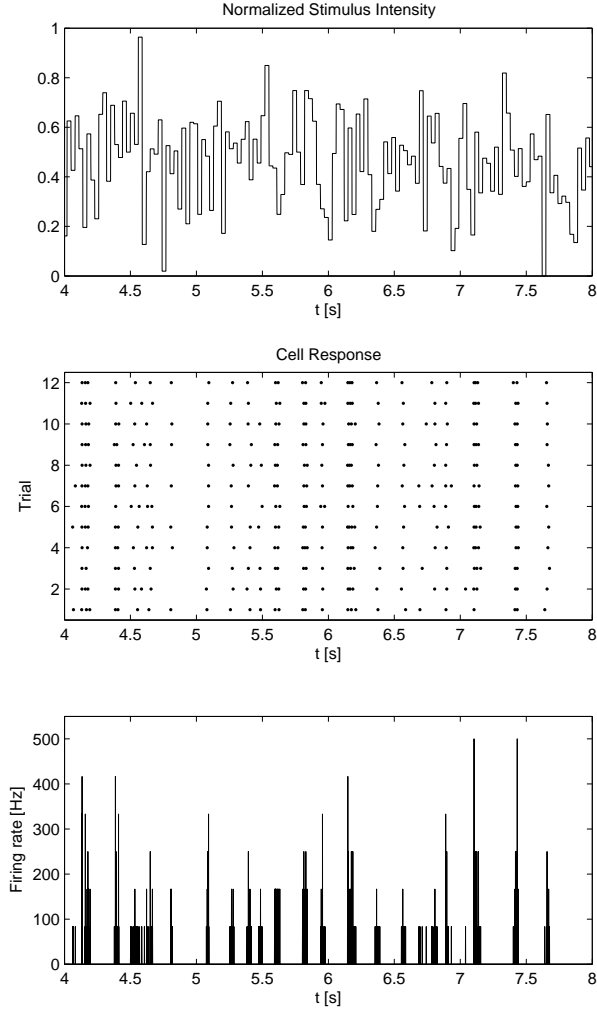


Figure 3. Firing events for a salamander retinal type-ON ganglion cell. *Top*: Stimulus intensity. *Middle*: Observed spike sequences. *Down*: Firing rate  $r(t)$ .

where the distorted sinus functions

$$f_j(t) = \begin{cases} \sin\left(\pi j\left(2\frac{t}{\tau_F} - \left(\frac{t}{\tau_F}\right)^2\right)\right) & 0 \leq t \leq \tau_F \\ 0 & \text{otherwise} \end{cases} \quad (10)$$

were used as basis functions to synthesize the filter, requiring a lower number of them to produce the filter accurately than if it is used a Fourier series representation. This filter impulse response has high amplitude near the origin and then decays rapidly, having a time duration given by  $\tau_F$ .

The signal  $g(t)$  results from convolving the stimulus  $s(t)$  with the filter  $F(t)$ :

$$g(t) = \int_{-\infty}^t s(\tau)F(t-\tau)d\tau \quad (11)$$

The model uses 15 different components of the type (10) to synthesize  $F(t)$ , which corresponds to  $N = 15$

in equation (9). This filter selects when the firing events will occur, since the signal  $g(t)$  will be stronger when the visual stimulus follows a pattern similar to the filter response. Afterwards, the generator potential  $g(t)$  is summed with a noise component  $a(t)$  and with a feedback signal  $p(t)$ , resulting in  $h(t)$ .

Then a threshold function, composed of three main parts, is applied to  $h(t)$ . First,  $h(t)$  is compared with a threshold level  $\theta$ , which is equivalent to  $\delta(h(t) - \theta)$ . In order to be fired only one spike, when the signal crosses the threshold in the upward direction, a second term of the form  $H(\dot{h}(t))$  is included, where the dot above  $h(t)$  is the Lagrangian notation for the signal derivative with respect to time. The first two blocks of the model, the filter  $F(t)$  and the threshold block, are intended to predict the time occurrence of the firing events, corresponding to make  $a(t) = b(t) = P(t) = 0$  in the model depicted in Figure 2.

In order to predict a correct number of firing events a feedback block that resembles the ganglion cell refractoriness after a firing event is included in the model. Each fired spike triggers a negative after-potential  $P(t)$ , with the form:

$$P(t) = B e^{-t/\tau_p} \quad (12)$$

that is added to the generator potential  $g(t)$  lowering the signal  $h(t)$  immediately after a firing.

The after-potential makes the signal  $h(t)$  to drop below the threshold, and the probability of subsequent firing events will be reduced until the after-potential decay. But if  $g(t)$  continues to rise in such a way that it compensates the negative potential  $P(t)$  the model will fire again, making large excursions of  $g(t)$  leading to a train of several spikes. This negative feedback loop serves both to simulate repetitive firing, within a firing event, and to include refractoriness after a firing.

The feedback block input signal is given by:

$$r(t) = \delta(h(t) - \theta)\dot{h}(t)H(\dot{h}(t)) \quad (13)$$

where a third component is included in the threshold function such that the input of the potential block is proportional to the slope, or instant raise, of  $h(t)$ . After adding the feedback loop the generator potential is given by

$$h(t) = g(t) + a(t) + \int_{-\infty}^t r(\tau)(1+b(\tau))P(t-\tau)d\tau \quad (14)$$

The model's output spike train is a series of delta functions, described by

$$\rho(t) = \sum \delta(t - t_i) \quad (15)$$

coming about at times  $t_i$  whenever the generator potential  $h(t)$  crosses the threshold  $\theta$  from below. Equation (15) is termed the neural response function.

The gaussian noise sources,  $a(t)$  and  $b(t)$  (see Figure 2) are used to model the variability of the neural response to the same stimulus. This variability comprises the

Stochastic model parameters					
$\theta$	$\tau_p$ [ms]	$B$	$\sigma_a$	$\sigma_b$	$\tau_a$ [ms]
0.59	110	1.51	0.30	0.85	200

Table 1. Parameters values for the stochastic model. (See Section 2)

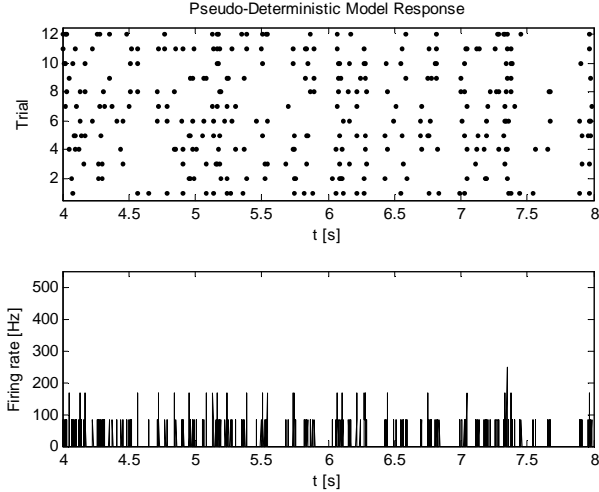


Figure 4. Pseudo-deterministic model response. *Top*: Spike-train sequences. *Down*: Firing rate  $r(t)$ .

variation of the total number of spikes and the drifting in its time occurrence.

The random signal  $a(t)$  has gaussian amplitude distribution, with zero mean and standard deviation  $\sigma_a$ , and an exponentially decaying autocorrelation function with time constant  $\tau_a$ . It is added to the generator potential  $g(t)$  causing random variability in the time occurrence of threshold crossing. Despite introducing some variability it is not sufficient to reproduce the neural response variability. Namely, the variability in the spike number remains lower than that observed in real neurons, and so another noise source  $b(t)$  was included in the model to modulate randomly the negative after-potential.  $b(t)$  has gaussian distribution with zero mean and standard deviation  $\sigma_b$  and a very short correlation time, so that its values are independent from spike to spike. These model parameters were obtained by optimizing the time occurrence of the first spike and the number of spikes, in a firing event.

### 3 Experimental Results

In order to compare results the used stimuli are spatially uniform, having only temporal information. In the case of the pseudo-deterministic model, the convolution of the spatial kernel with a spatially uniform stimulus is equivalent to directly multiply the stimulus by a constant factor and so it can be further ignored.

All filters were discretized in order to be suitable implemented in a digital computer. A portion (2s) of the used

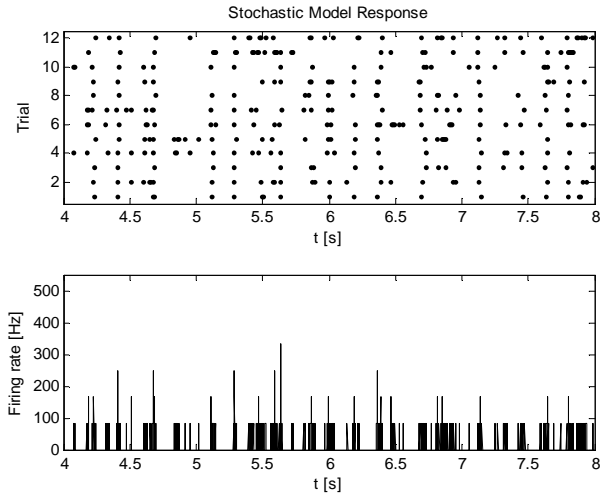


Figure 5. Stochastic model response. *Top*: Spike-train sequences. *Down*: Firing rate  $r(t)$ .

random stimulus is depicted in Figure 3, it was obtained by randomly sampling, every 30ms, a gaussian distribution with standard deviation equal to 35% of the mean level intensity ( $4mW/m^2$ ) [9]. This stimulus was used to excite both models and the results were compared with real spike trains, observed from 12 different experimental trials from a salamander retina. The stimulus has a temporal duration of 10s, and the results were averaged over this time period.

The models parameters used in the simulations are displayed in Table 2, for the pseudo-deterministic model, and in Table 1 for the stochastic model, respectively. Figures 4 and 5 show the models response, for 12 different experiments, in terms of spike trains and firing rate, computed by histogramming the 12 experiments using a time bin of width 1ms.

In order to study the models performances different error measures were used: (a) percentage of predicted spikes against the number of observed spikes given by the retina; (b) a spike train metric, to compare directly the spike trains sequences generated by the models with the real ones; and finally (c) a mean squared error measure, between the firing rate produced by the models and the one calculated from the real spike trains.

#### 3.1 Predicted Number of Spikes Error

The percentage of the predicted number of spikes relative to the number of observed spikes in an experimental trial is plotted, in Figure 6, against the number of spikes within an observed trial.

To calculate the error percentage of the predicted number of spikes, the number of spikes,  $N_{jP}$ , in each predicted sequence  $j$  was calculated formerly as:

$$N_{jP} = \int \rho_{jP}(t) dt \quad (16)$$

( $\rho(t)$  is the neural response function - equation (15)), and

Pseudo-deterministic model parameters								
$w_C$	$w_S$	$\sigma_C [\mu m]$	$\sigma_S [\mu m]$	$\alpha [Hz]$	$B [Hz]$	$\tau [ms]$	$\tilde{\alpha} [Hz]$	$\Theta$
3	$0.8w_C$	80	$3\sigma_C$	4	78	170	79	0.005

Table 2. Parameters values for the pseudo-deterministic model. (See Section 2)

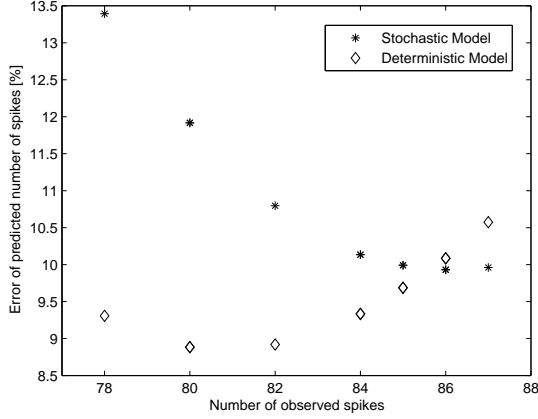


Figure 6. Percentage error in the predicted number of spikes.

	Pseudo-deterministic	Stochastic	Real
$\mu$	79.89	86.03	83.42
$\sigma$	8.89	10.92	2.81

Table 3. Mean and standard deviation for the number of spikes.

after that the following quantity is computed

$$\frac{|N_{jP} - N_{iO}|}{N_{iO}} \times 100\% \quad (17)$$

where  $N_{iO}$  is the number of spikes in the observed experimental trial  $i$ . The values given by equation (17) were averaged for all 300 model generated spike trains, and the result is plotted against  $N_{iO}$  in Figure 6, where the index  $i$  corresponds to the different real observed trials.

Table 3 presents some statistical parameters for the number of predicted and observed spikes trains. The mean and standard deviation were obtained using 300 runs of each model. The statistics for the observed number of spikes were computed using the 12 experimental trials. Both models predict well the mean number of spikes within a trial, reflected in their similar mean values. However the standard deviations are quite different for the models and real experiments.

The graph in Figure 6 shows the models behavior respective to the percentage error in the predicted number of spikes. The pseudo-deterministic model have a smaller error for a small number of spikes in the trials, and then increase. The stochastic model has an opposed behavior,

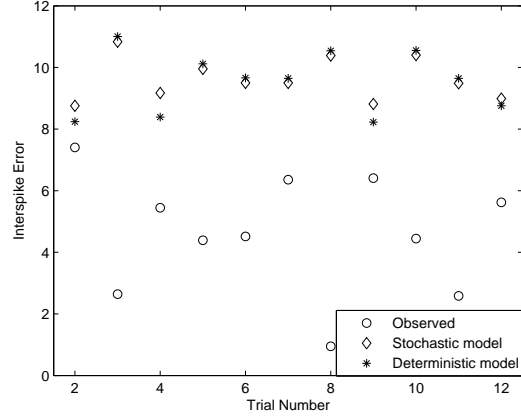


Figure 7. Inter-spike errors for the observed and generated spike trains

having big errors for small number of spikes in real trials and then decreases. As expected, due to the proximity of their means, both model's curves intersect for a number of observed spikes near their mean.

### 3.2 Spike Train Metric Error

Due to its discrete nature, two different spike trains, represented by equation (15), are not suitable to be compared using, for example, a mean-squared error (MSE). If one compares a spike train generated by one of the models with another one experimentally observed using the mean-squared error the spikes occurrence times must match exactly to have a small error or it would be better that the model didn't fire any spike at all, which is contradictory. Therefore, it was used a metric that calculates the cost of transforming one spike train into another using a set of basic operations: the deletion of spikes, which have a cost of  $p$  per spike, the generation of spikes, which have the same cost  $p$  per spike, and the time interval between spikes occurrence in each trial, with a cost  $q$  per second [13].

The graph in Figure 7 displays the inter-spike errors for the models and observed spike trains against the number of the observed trial for  $p = 1(\text{spike}^{-1})$  and  $q = 0.0001(\text{s}^{-1})$ . The observed inter-spike errors were calculated by taking a real observed spike train, for the case was the one observed in the first trial, and measuring its distance to every other observed spike train. For each model 11 runs were generated and the mean value of its inter-spike errors relative to the observed trial plotted.

From Figure 7 it can be seen that for the specific used

costs both models give similar errors, with the pseudo-deterministic model performing slightly better. It can also be seen that the variability between the first real trial and the other eleven real trials give margin for an improvement of the retina models.

### 3.3 Mean Squared Error

The mean squared error (MSE) is used to evaluate the models performance relatively to the firing rate. This measure is defined by [5]

$$E = \frac{\int (r_m(t) - r(t))^2 dt}{\int (r(t) - \bar{r})^2 dt} \quad (18)$$

where  $r_m(t)$  is the firing rate produced by the model  $m$ , and  $r(t)$  is the firing rate obtained from the peristimulus time histogram (PSTH) calculated from the observed real data by histogramming the spike times occurrence from all experimental trials, and dividing its amplitude by the width of the time bin and by the total trial's number. Formally, it is given by

$$r(t) = \frac{1}{M} \frac{\int_{t_1}^{t_2} \rho(t) dt}{t_2 - t_1} \quad (19)$$

in the time interval  $(t_1, t_2)$ ;  $M$  is the number of trials.

The MSE for the firing rate of the pseudo-deterministic model, given by equation (8), and the retina output firing rate is: 1.1075. While the MSE for the firing rate of the stochastic model, obtained by generating twelve spike trains with the model and calculating the resulting firing rate, was: 1.1309. Not surprisingly the pseudo-deterministic model performs better again since it was optimized to approximate the ganglion cell firing rate.

## 4 Conclusions

The present results point out that the pseudo-deterministic and stochastic retina models approximate the real neural retina response with good accuracy.

This preliminary experimental work shows that the simpler pseudo-deterministic model provides results not worse than the more elaborated stochastic model, what is not an obvious statement, and further experimental analysis have to be done. However, if further experiments confirm these results it can be concluded that there is no advantage of using more computational power to compute the stochastic model.

Another important conclusion that can be derived from this study is that there is a big margin of work to improve retina models since the error measures taken are bigger than the ones obtained by comparison of groups of different real retina data.

## 5 Acknowledgments

The experimental data used in this paper was gently provided by Prof. Markus Meister.

## References

- [1] F. Rieke, D. Warland, R. de Ruyter van Steveninck, and W. Bialek. *Spikes: Exploring the Neural Code*. (The MIT Press, Cambridge, Massachusetts, 1997).
- [2] M.J. Schnitzer and M. Meister. Multineuronal firing patterns in the signal from eye to brain. *Neuron*, 37:499–511, February 2003.
- [3] B. Agüera y Arcas, A.L. Fairhall, and W. Bialek. What can a single neuron compute? In Todd K. Leen, Thomas G. Dietterich, and Volker Tresp, editors, *Advances in Neural Information Processing Systems 13*, pages 75–81. MIT Press, 2001.
- [4] W. Bialek, F. Rieke, R. de Ruyter van Steveninck, and S. Warland. Reading a neural code. *Science*, 252:1854–1857, June 1991.
- [5] M.J. Berry II and M. Meister. Refractoriness and neural precision. *The Journal of Neuroscience*, 18(6):2200–2221, March 1998.
- [6] M.J. Berry, D.K. Warland, and M. Meister. The structure and precision of retinal spike trains. *Neurobiology, Proc. Natl. Acad. Sci. USA*, 94:5411–5416, May 1997.
- [7] M. Meister and M.J. Berry II. The neural code of the retina. *Neuron*, 22:253–450, March 1999.
- [8] S.D. Wilke, A. Thiel, C.W. Eurich, M. Greschner, M. Bongard, J. Ammermüller, and H. Schwegler. Population coding of motion patterns in the early visual system. *Journal of Comparative Physiology A: Sensory, Neural, and Behavioral Physiology*, 187(7):549–558, September 2001.
- [9] J. Keat, P. Reinagel, R.C. Reid, and M. Meister. Predicting every spike: A model for the responses of visual neurons. *Neuron*, 30:803–817, June 2001.
- [10] B.A. Wandell. *Foundations of Vision*. (Sinauer Associates, Sunderland, Massachusetts, 1995).
- [11] M.J. Berry II, I.H. Brivanlou, T.A. Jordan, and M. Meister. Anticipating of moving stimuli by the retina. *Nature*, 398:334–338, March 1999.
- [12] P. Dayan and L.F. Abbot. *Theoretical Neuroscience: Computational and Mathematical Modeling of Neural Systems*. (The MIT Press, Cambridge, Massachusetts, 2001).
- [13] J.D. Victor and K.P. Purpura. Nature and precision of temporal coding in visual cortex: A metric-space analysis. *Journal of Physiology*, 76(2):1310–1326, August 1996.